Ergodic Capacity Analysis of MISO/SIMO-OFDM with Arbitrary Antenna and Channel Tap Correlation

V.K. Varma Gottumukkala, *Student Member, IEEE*, Hlaing Minn, *Senior Member, IEEE*

***Abstract*—We analyze the ergodic capacity of MISO/SIMO-OFDM systems with arbitrary antenna and channel tap correlations. Existing works in literature consider the Kronecker model of antenna and channel tap correlations for capacity analysis. However, the applicability of such a model holds for not all practical scenarios. Here we assume a generalized correlation model and the Kronecker model is a special case of our model. We analyze the additional conditions beyond that needed by the Kronecker model for maximizing capacity and the ones that reduce capacity and derive a closed-form capacity expression. Our results are validated using Monte-Carlo simulations.**

***Index Terms*—MISO, SIMO, OFDM, Capacity, Correlation**

I. Introduction

Multi-antenna systems like multiple input multiple output (MIMO), multiple input single output (MISO), and single input multiple output (SIMO) along with orthogonal frequency division multiplexing (OFDM) are popularly used for improving different aspects of communication systems like channel capacity, diversity and bit error rates. The channel capacity has been among the most important performance metrics to characterize these systems.

The capacity of multi-antenna systems for spatially uncorrelated channels with uncorrelated taps (in delay domain) was found in [1] while [2] and [3] dealt with finding the capacity assuming transmit and/or receive antenna correlation in a flat fading MIMO channel. The capacity under antenna and channel tap correlation in frequency selective channels was considered in [4]. In the above works as well as other existing works in literature where an exact closed-form solution for the ergodic capacity is obtained, the correlation model considered is the so called Kronecker model where the transmit, receive and tap correlations can be decoupled. While it has been shown in [5], [6] that this model holds in many cases, still in practical scenarios, there can be cases where this model does not hold [7], [8]. According to [8], the Kronecker model predicts lower capacity particularly when there exists considerable correlation at the transmit and/or receive antenna ends. In [9], the authors considered a generalized correlation model for capacity analysis (without a closed-form capacity expression) and performed capacity analysis under large number of transmit and receive antennas approximation or for medium number of receive antennas under an approximation on the eigenvalues.

Several recent works have focussed on other aspects of capacity - these include capacity under Rician channel models [10]–[12], capacity under space time codes [13], the effect of interference on multi-antenna networks [14], capacity under per-antenna power constraint [15], [16], capacity under quality of service constraint [17], capacity under analog imperfections [18] and secrecy capacity [19] to name a few. Capacity analysis while using Kronecker model of correlation was done using character expansions in [20]. In [21], an asymptotic approach was used to find the covariance matrix for achieving capacity under Kronecker channel model.

In this work, we consider a general case of antenna and tap correlation under frequency-selective Rayleigh fading channels. We analyze the capacity expression at high and low SNR regimes for arbitrary number of transmit/receive antennas for MISO/SIMO-OFDM respectively, and find the closed-form capacity expression for all SNR regions. In deriving the above capacity expression, we utilize the probability density function (pdf) of a sum of weighted chi-square random variables which was developed in [22]. In [22], the authors dealt with carrier frequency offset estimation without any capacity analysis, whereas the current work focuses on the ergodic capacity analysis of a MISO/SIMO-OFDM system with arbitrary correlation. The case of same tap correlations for all antenna pairs which is a common model in existing works is a special case of our model. Due to the general nature of our analysis, all correlation possibilities that can exist in MISO/SIMO frequency selective channels are included in our model.

Notations: (i) bold font: vector/matrix, (ii) regular font: scalar, (iii) $(\cdot)^T$, $(\cdot)^H$: transpose and hermitian respectively, (iv) $|(\cdot)|$: denotes the absolute value if operated on a complex number and the cardinality if operated upon a set, (v) $\boldsymbol{I}_N$: the identity matrix of size N, (vi) $\boldsymbol{0}_{N_1\times N_2}$: all zeros matrix of size $N_1 \times N_2$, (vii) $\mathcal{CN}(\boldsymbol{m}, \boldsymbol{C})$: complex Gaussian with mean vector $\boldsymbol{m}$ and covariance matrix $\boldsymbol{C}$, (viii) i.i.d.: independent and identically distributed, (ix) $\mathrm{tr}\{\boldsymbol{A}\}$: trace of matrix $\boldsymbol{A}$, (x) $\otimes$: Kronecker product, (xi) $(\cdot)!$ denotes factorial, (xii) $\mathrm{diag}\left\{\boldsymbol{A}_i\right\}_{i=i_1}^{i_n}$: a block diagonal matrix with matrices $\boldsymbol{A}_{i_1}, \ldots, \boldsymbol{A}_{i_n}$ on the block diagonal locations, (xiii) $\log$: logarithm to base 2 and (xiv) $\ln$: natural logarithm.

II. System Model

We consider a MISO-OFDM system with M transmit antennas or a SIMO-OFDM system with M receive antennas and N subcarriers. We use N_T to denote the number of transmit antennas; thus $N_T = M$ for MISO-OFDM and $N_T = 1$ for SIMO-OFDM. Let $h_i^{(l)}$ denote the lth tap channel gain corresponding to the ith transmit antenna for MISO-OFDM and the ith receive antenna for SIMO-OFDM. Let L be the maximum of the number of channel taps among

The authors are with The Department of Electrical Engineering, University of Texas at Dallas, Richardson, Texas 75080. Email: {vkg071000, Hlaing.Minn}@utdallas.edu.

the various transmit-receive antenna pairs. Then we define $\boldsymbol{h}_i = [h_i^{(0)}, h_i^{(1)}, \ldots, h_i^{(L-1)}]^T$, $\boldsymbol{h}^{(l)} = [h_1^{(l)}, h_2^{(l)}, \ldots, h_M^{(l)}]^T$ and $\boldsymbol{H} = [\boldsymbol{h}^{(0)T}, \boldsymbol{h}^{(1)T}, \ldots, \boldsymbol{h}^{(L-1)T}]^T$.

In our model, the channel autocorrelation matrix $\boldsymbol{R}_H \triangleq E[\boldsymbol{H}\boldsymbol{H}^H]$ can have arbitrary entries as long as it is a valid autocorrelation matrix. In contrast, the Kronecker model is of the specific form $\boldsymbol{R}_H = \boldsymbol{R}_{\text{tap}} \otimes \boldsymbol{R}_{\text{T}}^T$ for MISO and $\boldsymbol{R}_H = \boldsymbol{R}_{\text{tap}} \otimes \boldsymbol{R}_{\text{R}}$ for SIMO where $\boldsymbol{R}_{\text{tap}} = \text{E}[\boldsymbol{h}_i \boldsymbol{h}_i^H], i = 1, \ldots, M$ and $\boldsymbol{R}_{\text{T}} = \boldsymbol{R}_{\text{R}} = \text{E}[\boldsymbol{h}^{(l)} \boldsymbol{h}^{(l)H}], l = 0, \ldots, L-1$. Let $\boldsymbol{F}$ be the $N \times N$ unitary Discrete Fourier Transform (DFT) matrix, $\boldsymbol{F}_L$ the matrix with the first L columns of $\boldsymbol{F}$, $\boldsymbol{F}_{L,k}$ the kth row of $\boldsymbol{F}_L$ and $\boldsymbol{f}_k$ the kth row of $\boldsymbol{F}$. Let $H_{i,k} = \sqrt{N}\boldsymbol{F}_{L,k}\boldsymbol{h}_i$ denote the channel gain on the kth tone of channel $\boldsymbol{h}_i$, where factor $\sqrt{N}$ arises due to our definition of $\boldsymbol{F}$ as the unitary DFT matrix. Define $\boldsymbol{H}_k = [H_{1,k}, H_{2,k}, \ldots, H_{M,k}]^T$ as the kth tone MISO/SIMO channel vector. Then, $\boldsymbol{H}_k = \sqrt{N}[\boldsymbol{F}_{L,k} \otimes \boldsymbol{I}_M]\boldsymbol{H}$ and

$$\boldsymbol{R}_{H_k} = E[\boldsymbol{H}_k \boldsymbol{H}_k^H] = N[\boldsymbol{F}_{L,k} \otimes \boldsymbol{I}_M]\boldsymbol{R}_H[\boldsymbol{F}_{L,k}^H \otimes \boldsymbol{I}_M]. \quad (1)$$

We use $\boldsymbol{x}_i$ to denote the $N \times 1$ time domain data vector at the ith transmit antenna ($i = 1$ for SIMO), $X_{i,k}$ the corresponding kth tone data symbol and $\boldsymbol{X}_k \triangleq [X_{1,k}, X_{2,k}, \ldots X_{N_T,k}]^T$.

For MISO-OFDM, after cyclic prefix removal, we can write the received signal vector as

$$\boldsymbol{y} = [\boldsymbol{H}_{(1)}, \boldsymbol{H}_{(2)}, \ldots, \boldsymbol{H}_{(M)}] \left[\boldsymbol{x}_1^T, \boldsymbol{x}_2^T, \ldots, \boldsymbol{x}_M^T\right]^T + \boldsymbol{w} \quad (2)$$

where $\boldsymbol{H}_{(i)}$ is the convolution matrix (circulant) corresponding to $\boldsymbol{h}_i$ with the first row being $[\boldsymbol{h}_i^T, \boldsymbol{0}_{1\times(N-L)}]$ and each of the remaining rows right shifted circularly by one position relative to the previous row and $\boldsymbol{w}$ is distributed as $\mathcal{CN}(\boldsymbol{0}_{N\times 1}, \sigma_w^2 \boldsymbol{I}_N)$. Taking DFT on (2) gives

$$Y_k = \boldsymbol{H}_k^T \boldsymbol{X}_k + W_k, \quad k = 0, 1, \ldots, N-1 \quad (3)$$

where $Y_k = \sqrt{N}\boldsymbol{f}_k \boldsymbol{y}$ and $W_k = \sqrt{N}\boldsymbol{f}_k \boldsymbol{w}$ are the received signal and noise on the kth tone.

For SIMO-OFDM, we have

$$\boldsymbol{Y}_k = \boldsymbol{H}_k X_{1,k} + \boldsymbol{W}_k \quad (4)$$

where $\boldsymbol{Y}_k = \sqrt{N}[\boldsymbol{f}_k \boldsymbol{y}_1, \ldots, \boldsymbol{f}_k \boldsymbol{y}_M]^T$ and $\boldsymbol{W}_k = \sqrt{N}[\boldsymbol{f}_k \boldsymbol{w}_1, \ldots, \boldsymbol{f}_k \boldsymbol{w}_M]^T$ with $\boldsymbol{y}_i$ and $\boldsymbol{w}_i$ being the $N \times 1$ time domain received vector and noise vector at the ith receive antenna, respectively.

For both MISO-OFDM and SIMO-OFDM, we stack the received signal/vector over all tones and write as

$$\bar{\boldsymbol{Y}} = \bar{\boldsymbol{H}}^T \bar{\boldsymbol{X}} + \bar{\boldsymbol{W}} \quad \text{(for MISO-OFDM)} \quad (5)$$

$$\bar{\boldsymbol{Y}} = \bar{\boldsymbol{H}} \bar{\boldsymbol{X}} + \bar{\boldsymbol{W}} \quad \text{(for SIMO-OFDM)} \quad (6)$$

where $\bar{\boldsymbol{Y}} \triangleq [\boldsymbol{Y}_1^T, \boldsymbol{Y}_2^T, \ldots, \boldsymbol{Y}_{N-1}^T]^T$, $\bar{\boldsymbol{X}} \triangleq [\boldsymbol{X}_1^T, \boldsymbol{X}_2^T, \ldots, \boldsymbol{X}_{N-1}^T]$, $\bar{\boldsymbol{W}} \triangleq [\boldsymbol{W}_1^T, \boldsymbol{W}_2^T, \ldots, \boldsymbol{W}_{N-1}^T]^T$ and we define the $NM \times N$ block diagonal matrix $\bar{\boldsymbol{H}} \triangleq \text{diag}\{\boldsymbol{H}_k\}_{k=0}^{N-1}$. We note that for MISO-OFDM case, $\boldsymbol{Y}_k$ and $\boldsymbol{W}_k$ in the above definition are scalars, and hence equal to Y_k and W_k respectively and for SIMO-OFDM case, $\boldsymbol{X}_k$ is a scalar and hence equal to $X_{1,k}$.

III. Ergodic Channel Capacity

When the channel is unknown at the transmitter, the capacity of this system is achieved for i.i.d. circularly symmetric complex Gaussian input symbols, i.e., equal power must be allocated at all transmit antennas and across all tones [1], [23], [24]. Then $\bar{\boldsymbol{X}} \sim \mathcal{CN}(\boldsymbol{0}_{N_d N_T \times 1}, \frac{P_X}{N_T}\boldsymbol{I}_{N_d N_T})$, where $P_X = E[\boldsymbol{X}_k^H \boldsymbol{X}_k]$, $k \in \mathcal{I}$, is the average total transmit energy on a data tone, $\mathcal{I}$ denotes the set of data tones and $N_d \triangleq |\mathcal{I}|$. Then, the ergodic capacity (normalized per OFDM subcarrier) for MISO/SIMO-OFDM systems can be written as [4], [9]

$$C = \frac{1}{N}\text{E}\left[\log\left\{\det\left(\boldsymbol{I}_{N_d} + \frac{\bar{\boldsymbol{H}}_d^H \bar{\boldsymbol{H}}_d}{\rho}\right)\right\}\right] \quad (7)$$

where $\bar{\boldsymbol{H}}_d \triangleq \text{diag}\{\boldsymbol{H}_k\}_{k\in\mathcal{I}}$ is similar to $\bar{\boldsymbol{H}}$ but consists of only the channel vectors corresponding to the data tones and $\rho \triangleq \frac{N_T N \sigma_w^2}{P_X}$. Noting that $\boldsymbol{I}_{N_d} + \frac{\bar{\boldsymbol{H}}_d^H \bar{\boldsymbol{H}}_d}{\rho}$ is a diagonal matrix, we can simplify the above as

$$C = \frac{1}{N}\sum_{k\in\mathcal{I}} \text{E}\left[\log\left(1 + \frac{\boldsymbol{H}_k^H \boldsymbol{H}_k}{\rho}\right)\right]. \quad (8)$$

Let $\boldsymbol{R}_{H_k} = \boldsymbol{U}_k \boldsymbol{\Sigma}_k \boldsymbol{U}_k^H$ be the "truncated" eigenvalue decomposition of $\boldsymbol{R}_{H_k}$ (which has rank r_k). Here $\boldsymbol{\Sigma}_k$ is a diagonal matrix with only the non-zero eigenvalues of $\boldsymbol{R}_{H_k}$ as its diagonal entries, $\boldsymbol{U}_k$ consists of the first r_k columns of the unitary matrix taken from a standard eigenvalue decomposition of $\boldsymbol{R}_{H_k}$ and $\boldsymbol{U}_k^H \boldsymbol{U}_k = \boldsymbol{I}_{r_k}$. Thus, $\boldsymbol{H}_k$ can be expressed as $\boldsymbol{H}_k = \boldsymbol{U}_k \boldsymbol{\Sigma}_k^{\frac{1}{2}} \tilde{\boldsymbol{H}}_k$ where the $r_k \times 1$ vector $\tilde{\boldsymbol{H}}_k$ consists of i.i.d. $\mathcal{CN}(0,1)$ entries. Using this result in (8) gives

$$C = \frac{1}{N}\sum_{k\in\mathcal{I}} \text{E}\left[\log\left(1 + \frac{\tilde{\boldsymbol{H}}_k^H \boldsymbol{\Sigma}_k \tilde{\boldsymbol{H}}_k}{\rho}\right)\right]. \quad (9)$$

We now analyze this expression in high and low SNR regimes where $\text{SNR} \triangleq \frac{P_X}{N\sigma_w^2}$.

A. High SNR:

At high SNR, we can approximate (9) as

$$C \approx \frac{1}{N}\sum_{k\in\mathcal{I}} \text{E}\left[\log\left(\frac{\tilde{\boldsymbol{H}}_k^H \boldsymbol{\Sigma}_k \tilde{\boldsymbol{H}}_k}{\rho}\right)\right] \quad (10)$$

$$= \frac{1}{N}\sum_{k\in\mathcal{I}} \text{E}\left[\log\left(\frac{\sum_{i=1}^{r_k} \lambda_{k,i} |[\tilde{\boldsymbol{H}}_k]_i|^2}{p}\right)\right] \quad (11)$$

where $[\tilde{\boldsymbol{H}}_k]_i$ is the ith element of vector $\tilde{\boldsymbol{H}}_k$ and $\lambda_{k,i}$ is the ith diagonal element of $\boldsymbol{\Sigma}_k$. Noting that $\tilde{\boldsymbol{H}}_k$ consists of $\mathcal{CN}(0,1)$ entries, the $\log$ term in the right-hand side (RHS) of (11) is symmetric about $\lambda_{k,i}, i = 1, 2, ...r_k$, since reordering these eigenvalues does not change the result. Also the term is a joint concave function over $\lambda_{k,i}, i = 1, 2, ..., r_k$. Under the constraint that $\text{tr}\{\boldsymbol{\Sigma}_k\} = \text{tr}\{\boldsymbol{R}_{H_k}\}$ is constant, uniform eigenvalues maximize the $\log$ term in RHS of (11) [4], [25].

Therefore, if we denote the uniform eigenvalues of $\boldsymbol{\Sigma}_k$ as $\lambda_{k,1} = \lambda_{k,2} = ... = \lambda_{k,r_k} = \frac{\text{tr}(\boldsymbol{\Sigma}_k)}{r_k} \triangleq \lambda_k$, and the

corresponding capacity by C_1, then from (11) we have,

$$C_1 \triangleq \frac{1}{N}\sum_{k\in\mathcal{I}} \mathrm{E}\left[\log\left(\frac{\tilde{\boldsymbol{H}}_k^H\tilde{\boldsymbol{H}}_k}{\rho}\right)\right] + \frac{1}{N}\sum_{k\in\mathcal{I}}\left[\log\left(\frac{\mathrm{tr}(\boldsymbol{\Sigma}_k)}{r_k}\right)\right]. \quad (12)$$

The first term of (12) can be simplified further as follows:

$$\mathrm{E}\left[\log\left(\frac{\tilde{\boldsymbol{H}}_k^H\tilde{\boldsymbol{H}}_k}{\rho}\right)\right] = \mathrm{E}\left[\log(v_k)\right] - \log(\rho) \quad (13)$$

where $v_k \triangleq \tilde{\boldsymbol{H}}_k^H\tilde{\boldsymbol{H}}_k$ is a central Chi-square random variable with $2r_k$ degrees of freedom and its pdf is $f_{v_k}(v) = \frac{1}{\Gamma(r_k)}v^{r_k-1}e^{-v}, v\geq 0$, where $\Gamma(n) = (n-1)!$ is the Gamma function. Therefore,

$$\mathrm{E}[\log(v_k)] = \log(e)\int_0^\infty \frac{1}{\Gamma(r_k)}v^{r_k-1}e^{-v}\ln(v)dv = \psi(r_k)\log(e) \quad (14)$$

where $\psi(r_k)$ is the Euler's psi function given as $\psi(k+1) = -c + \sum_{n=1}^{k}\frac{1}{n}$ and $c = 0.577215$ is the Euler's constant [26, 4.352-1,8.365-4]. Using these results, we can rewrite (12) as

$$C_1 \triangleq \frac{\log(e)}{N}\sum_{k\in\mathcal{I}}[\psi(r_k) - \ln(r_k) - \ln(\rho)] + \frac{\log(e)}{N}\sum_{k\in\mathcal{I}}[\ln(\mathrm{tr}(\boldsymbol{\Sigma}_k))]. \quad (15)$$

For any given k and $\boldsymbol{\Sigma}_k$, we can show that $\psi(r_k) - \ln(r_k)$ increases for increasing r_k (details in Appendix A) and thus it is maximum when r_k is maximum, i.e., equal to full rank.

For the capacity-maximizing r_k, i.e., maximum r_k, the first summation term on RHS of (15) is independent of the correlation. So we need to find the correlation that maximizes the second term to maximize C_1. Using Jensen's inequality on the second term, we have

$$\frac{1}{N}\sum_{k\in\mathcal{I}}\ln(\mathrm{tr}(\boldsymbol{\Sigma}_k)) \leq \frac{|\mathcal{I}|}{N}\left[\ln\left(\frac{1}{|\mathcal{I}|}\sum_{k\in\mathcal{I}}\mathrm{tr}(\boldsymbol{\Sigma}_k)\right)\right] \quad (16)$$

with the equality obtained when $\mathrm{tr}(\boldsymbol{\Sigma}_k)$ remains the same for all k. Since we found earlier that r_k should be equal to full rank value for all k and λ_k's for each k should be equal, constant $\mathrm{tr}(\boldsymbol{\Sigma}_k)$ for all k results in $\lambda_k = \frac{\mathrm{tr}(\boldsymbol{\Sigma}_k)}{r_k}$ being the same for all k. From (1), we see that when $\mathrm{tr}\{\boldsymbol{R}_H\}$ is kept constant, equal eigenvalues for $\boldsymbol{\Sigma}_k, \forall k$ are obtained when $\boldsymbol{R}_H$ is diagonal and $\sum_{i=0}^{L-1}\boldsymbol{R}_H(j+iN_T, j+iN_T) = \text{constant}, \forall j$. Under constraint $\mathrm{tr}\{\boldsymbol{R}_H\} = \text{constant}$ and from (1), diagonal $\boldsymbol{R}_H$ results in constant $\mathrm{tr}\{\boldsymbol{\Sigma}_k\}$ while arbitrary $\boldsymbol{R}_H$ results in constant $\sum_{k=0}^{N-1}\mathrm{tr}\{\boldsymbol{\Sigma}_k\}$. This implies that capacity is maximized for uncorrelated antenna and channel taps and when the sum of energies in all the channel taps is the same for all antenna pairs. From [4], we know that under the Kronecker model of antenna and tap correlation, capacity is maximized for uncorrelated taps and uniform eigenvalues of the antenna correlation matrix. Recall that the tap correlation and power delay profile is the same for all antenna pairs in the Kronecker model. Thus for the arbitrary correlation case, our new observation is that the capacity is maximized even for different tap energies (i.e. different power delay profiles) at each antenna pair as long as the taps are uncorrelated and the sum of energies in the taps is the same across all the antenna pairs.

We now consider the correlation that lowers capacity. When $\mathrm{tr}\{\boldsymbol{\Sigma}_k\}$ is constant, we expect that the $\log$ term in (11) reduces when the eigenvalues are non-uniform and is minimized when there is only a single non-zero eigenvalue. Furthermore, from Jensen's inequality, $\frac{1}{N}\sum_{k\in\mathcal{I}}[\log(\lambda_k)]$ is lower when the single non-zero eigenvalue is different for different k. Note that having a diagonal $\boldsymbol{R}_H$ with a single non-zero entry results in a single non-zero eigenvalue for each $\boldsymbol{\Sigma}_k$, and the non-zero eigenvalue is the same for all k. However, for $\boldsymbol{R}_H$ equal to the Kronecker model with $(\rho_{\mathrm{tap}}, \rho_{\mathrm{T}}) = (1,1)$, $\boldsymbol{\Sigma}_k$ has a single non-zero eigenvalue which is different for different k resulting in a lower capacity than the previous case. In general, for arbitrary $\boldsymbol{R}_H$ and with $|\mathcal{I}| \approx N$, the constraint $\mathrm{tr}\{\boldsymbol{R}_H\} = \text{constant}$ translates to constant $\sum_{k\in\mathcal{I}}\mathrm{tr}\{\boldsymbol{R}_{H_k}\} = \sum_{k\in\mathcal{I}}\mathrm{tr}\{\boldsymbol{\Sigma}_k\}$, instead of constant $\mathrm{tr}\{\boldsymbol{\Sigma}_k\}$ and thus it is not exactly known what distribution of energies between all the eigenvalues over all k will absolutely minimize the capacity. Moreover, under constant $\mathrm{tr}\{\boldsymbol{R}_H\}$ and $|\mathcal{I}| < N$, $\sum_{k\in\mathcal{I}}\mathrm{tr}\{\boldsymbol{\Sigma}_k\}$ is different for different correlation matrices and this difference also contributes to the difference in capacity.

B. Low SNR:

At low SNR, using the approximation $\log(1+x) \approx x\log(e)$ for small x and $\boldsymbol{A}^H\boldsymbol{A} = \mathrm{tr}\{\boldsymbol{A}\boldsymbol{A}^H\}$ for any column vector $\boldsymbol{A}$, we can approximate (8) as

$$\begin{aligned} C &\approx \frac{\log(e)}{\rho N}\sum_{k\in\mathcal{I}}\mathrm{E}\left[\mathrm{tr}\{\boldsymbol{H}_k\boldsymbol{H}_k^H\}\right] \\ &\approx \frac{\log(e)}{\rho}\mathrm{E}\left[\mathrm{tr}\{\frac{1}{N}\sum_{k=1}^{N}[\boldsymbol{f}_{L,k}^H\otimes\boldsymbol{I}_{N_T}][\boldsymbol{f}_{L,k}\otimes\boldsymbol{I}_{N_T}]\boldsymbol{H}\boldsymbol{H}^H\}\right] \\ &= \frac{\log(e)}{\rho}\mathrm{tr}\{\boldsymbol{R}_H\} \end{aligned} \quad (17)$$

where the approximation in the 2nd step was for $|\mathcal{I}| \approx N$, i.e., when most of the tones are used for data. When $|\mathcal{I}| << N$, (17) is an upper bound to the capacity.

From (17), we see that under constant $\mathrm{tr}\{\boldsymbol{R}_H\}$, all correlation cases yield the same capacity in the low SNR regime.

IV. Exact Capacity Expression

In this section, we derive the exact capacity expression for MISO/SIMO-OFDM systems with arbitrary correlation. In (9), $z_k \triangleq \tilde{\boldsymbol{H}}_k^H\boldsymbol{\Sigma}_k\tilde{\boldsymbol{H}}_k$ is the sum of weighted, i.i.d chi-square random variables whose pdf denoted by $p_{z_k}(z)$ can be obtained as in [22]. Then, (9) can be evaluated as

$$C = \frac{1}{N}\sum_{k\in\mathcal{I}}\int_{-\infty}^{\infty}\log\left(1+\frac{z}{\rho}\right)p_{z_k}(z)dz. \quad (18)$$

After evaluating this expression (details of which are provided in Appendix B), we obtain the following closed-form result for the ergodic capacity of the MISO/SIMO-OFDM system:[1]

$$C = \frac{1}{N}\sum_{k\in\mathcal{I}_1}\sum_{l=1}^{m}\sum_{i=1}^{\kappa_l}\frac{A_{li,k}}{\lambda_{l,k}^{i}\Gamma(i)}I_{li,k} + \frac{1}{N}\sum_{k\in\mathcal{I}_2}\frac{I_{1r_k,k}}{\Gamma(r_k)\lambda_{1,k}^{r_k}}, \quad \text{where} \tag{19}$$

$$I_{li,k} = \frac{\log(e)}{\rho}\sum_{j=1}^{i}\frac{(i-1)!}{(i-j)!}\lambda_{l,k}^{j}S_{ijl,k} \quad \text{and} \tag{20}$$

$$S_{ijl,k} = \rho e^{\frac{\rho}{\lambda_{l,k}}}\sum_{q=0}^{i-j-1}(-1)^q\binom{i-j}{q}\lambda_{l,k}^{i-j-q}\rho^q \times \left[\sum_{r=1}^{i-j-q}\left(\frac{\rho}{\lambda_{l,k}}\right)^{i-j-q-r}\frac{(i-j-q-1)!}{(i-j-q-r)!}e^{-\frac{\rho}{\lambda_{l,k}}}\right] + e^{\frac{\rho}{\lambda_{l,k}}}(-1)^{i-j}\rho^{i-j+1}\mathrm{E}_1\left(\frac{\rho}{\lambda_{l,k}}\right). \tag{21}$$

Here $A_{li,k}$ is defined similar to A_{li} in [22], with the additional index k used to denote its dependence on tone index k, $\mathrm{E}_1(x) \triangleq \int_x^\infty \frac{e^{-t}}{t}dt$ is the exponential integral, $\mathcal{I}_1$ and $\mathcal{I}_2$ are the subsets of $\mathcal{I}$ such that if $k \in \mathcal{I}_1$, $\boldsymbol{R}_{H_k}$ has at least two distinct eigenvalues and if $k \in \mathcal{I}_2$, $\boldsymbol{R}_{H_k}$ has all identical eigenvalues (i.e. a single non-zero eigenvalue with multiplicity r_k). For some tones $k \in \mathcal{J}_1 \subseteq \mathcal{I}_1$, if $\boldsymbol{R}_{H_k}$ consists of all distinct eigenvalues, then the first term in (19) can be further simplified as

$$\frac{1}{N}\sum_{k\in\mathcal{I}_1}\sum_{l=1}^{m}\sum_{i=1}^{\kappa_l}\frac{A_{li,k}}{\lambda_{l,k}^{i}\Gamma(i)}I_{li,k} = \tag{22}$$

$$\frac{1}{N}\sum_{k\in\mathcal{J}_1}\sum_{l=1}^{m}\frac{(-\lambda_{l,k})^{m-1}}{\Pi_{s=1,s\neq l}^{m}(\lambda_{s,k}-\lambda_{l,k})}e^{\frac{\rho}{\lambda_{l,k}}}\mathrm{E}_1(\frac{\rho}{\lambda_{l,k}}) + \frac{1}{N}\sum_{k\in\mathcal{I}_1\setminus\mathcal{J}_1}\sum_{l=1}^{m}\sum_{i=1}^{\kappa_l}\frac{A_{li,k}}{\lambda_{l,k}^{i}\Gamma(i)}I_{li,k}. \tag{23}$$

V. Performance Comparison

In Fig. 1, we compare the capacity results of SIMO-OFDM (using (19)) under various correlation scenarios with both arbitrary correlation and Kronecker models. For the Kronecker model, we used the exponential correlation model, i.e., the (i,j)th elements of the correlation matrices are selected as $\{\boldsymbol{R}_{\mathrm{tap}}\}_{i,j} = \sqrt{\gamma_i\gamma_j}\rho_{\mathrm{tap}}^{|i-j|}$ and $\{\boldsymbol{R}_T\}_{i,j} = \rho_T^{|i-j|}$ where $\gamma_l, \rho_{\mathrm{tap}}$ and ρ_T are the power in the lth tap, tap correlation and antenna correlation coefficient respectively. In the figure legend, we denote the Kronecker model with $(\rho_{\mathrm{tap}}, \rho_{\mathrm{T}})$ as "Kron $(\rho_{\mathrm{tap}}, \rho_{\mathrm{T}})$". From Fig. 1, we notice that three of the cases yield the maximum capacity (all these cases stack up on the topmost curve in the figure) among the compared scenarios: (i) diagonal $\boldsymbol{R}_H$ with all diagonal entries equal ("R_H, all same" on legend), (ii) diagonal $\boldsymbol{R}_H$ with non-uniform diagonal entries satisfying $\sum_{i=0}^{L-1}\boldsymbol{R}_H(j+iN_T, j+iN_T) = \text{constant}, \forall j$ ("R_H, sum same" on legend), and (iii) Kronecker model of $\boldsymbol{R}_H$ with $(\rho_{\mathrm{tap}}, \rho_{\mathrm{T}}) = (0,0)$. This is expected from our analysis since all these cases result in the uniform eigenvalues for $\boldsymbol{R}_{H_k}$ which are the same over the tone index k.

Next, we generate arbitrary entries for $\boldsymbol{R}_H$ ("R_H, unifrnd" on legend) by $\boldsymbol{R}_H = \frac{\boldsymbol{A}\boldsymbol{A}^H}{\mathrm{tr}\{\boldsymbol{A}\boldsymbol{A}^H\}}$ where entries of $LN_T \times LN_T$ matrix $\boldsymbol{A}$ are from i.i.d. uniform distribution between -1 and 1. In this case, despite the channels and taps being arbitrarily correlated, the capacity was quite close to the maximum capacity obtained with uncorrelated antennas and taps. The reason is that the eigenvalues were somewhat uniform despite the arbitrary correlation entries selected. Hence, as expected from our analysis, there was not much loss in the capacity. This shows us that it is possible to obtain near maximum capacity for correlation cases different from the well known uncorrelated scenario as long as there is not much variation in the eigenvalues.

Next, we see that as the correlation coefficients are increased in the Kronecker model, the capacity reduces, as expected from literature. The reason is that as ρ_{tap} and ρ_{T} are increased, the eigenvalues of $\boldsymbol{R}_{H_k}$ become less uniform with a few eigenvalues taking large values compared to all the remaining eigenvalues. From (1), the eigenvalues of $\boldsymbol{R}_{H_k}$ for a few extreme cases in the Kronecker model can be obtained as:

$$\mathrm{Kron}(1,0) : \lambda_{1,k} = \frac{N[\sum_{i=1}^{L}\boldsymbol{F}_{L,k,i}^{*}(\sum_{j=1}^{L}\boldsymbol{F}_{L,k,j}\sqrt{\gamma_i\gamma_j})]}{N_T\sum_{i=1}^{L}\gamma_i}, \quad \kappa_1 = N_T, m = 1, \tag{24}$$

$$\mathrm{Kron}(0,1) : \lambda_{1,k} = \frac{N[\sum_{i=1}^{L}|\boldsymbol{F}_{L,k,i}|^2\gamma_i]}{\sum_{i=1}^{L}\gamma_i}, \quad \kappa_1 = m = 1, \tag{25}$$

$$\mathrm{Kron}(1,1) : \lambda_{1,k} = \frac{N[\sum_{i=1}^{L}\boldsymbol{F}_{L,k,i}^{*}(\sum_{j=1}^{L}\boldsymbol{F}_{L,k,j}\sqrt{\gamma_i\gamma_j})]}{\sum_{i=1}^{L}\gamma_i}, \quad \kappa_1 = m = 1. \tag{26}$$

Here, $\boldsymbol{F}_{L,k,i}$ denotes the ith element of $\boldsymbol{F}_{L,k}$. Using these values in the second term of (12), we can directly evaluate which of these give a higher capacity. We notice that one of either "Kron $(1,0)$" and "Kron $(0,1)$" gives a better capacity depending on the relative values of N_T, L and choice of $\mathcal{I}$. The above eigenvalue expressions also allow us to evaluate whether tap correlation or antenna correlation is preferable in terms of capacity for the given system parameters.

Among the lower capacity curves, we notice that the Kronecker model with $(\rho_{\mathrm{tap}}, \rho_{\mathrm{T}}) = (1,1)$ yields the least capacity, lower than the case of $\boldsymbol{R}_H$ with all zero entries except for a single non-zero entry on the diagonal ("R_H, single non-zero diag entry" on legend). This is due to the single non-zero eigenvalue of $\boldsymbol{R}_{H_k}$ differing for different k in the former. This indicates that the capacity of a multi-antenna, frequency-selective system employing OFDM with all the channel energy concentrated in the single tap of a single antenna is better than the capacity of a similar system but with channel energy spread over all taps and antennas under full antenna and tap correlation.

In the low SNR region, all the correlation scenarios give quite close capacity values, as expected from our analysis.

[1]The evaluation of a similar integral is provided in terms of the complementary incomplete gamma function in [3]. Here we provide the solution in simpler terms without the need for this function.

Results for MISO-OFDM are shown in Fig. 2. We notice similar results for MISO-OFDM as in SIMO-OFDM.

In Fig. 3, we compare the capacity for MISO/SIMO-OFDM obtained from the derived analytical expression (19) and simulations (9) under arbitrary correlation. For each analytic and simulation pair, we use a different correlation matrix with arbitrary entries. We see that the analytic and simulation curves match perfectly for all SNR regions and for all correlation matrices, thereby proving the validity of our derived expression. From the MISO-OFDM curves corresponding to 2×1, 3×1 and 4×1 cases, we see a reduction in capacity with increasing number of antennas. This is because, we selected adverse correlation scenarios (non-uniform eigenvalues) with increasing antennas to study how degradation in capacity due to correlation compares with increase in capacity due to increase in number of antennas. From this figure, we see that adverse correlation scenarios can even negate the capacity advantages of increased antennas. However, if the correlation matrices for the three antenna cases are the same, we see increasing capacity with increasing number of antennas as is expected from literature. [2]

VI. Conclusions

A generalized correlation between antennas and channel taps in MISO/SIMO-OFDM systems was considered wherein we did not constrain the tap correlations for different transmit and receive antenna pairs to be the same and we analyzed the capacity and obtained a closed-form solution for the ergodic channel capacity that can be computed efficiently. We found the correlation scenarios that result in maximum capacity under arbitrary correlation case and discuss the correlation scenarios that reduce capacity. We observed that capacity is maximized even for different power delay profiles under uncorrelated antennas and taps as long as the sum of energies in all the taps is the same across all antenna pairs. Even for completely arbitrarily correlated antennas and taps, it was found possible to obtain near maximum capacity as long as the eigenvalues of the correlation matrix were nearly uniform.

Appendix A
Maximization of first summation term in (15)

Consider two values of $[\psi(r_k) - \ln(r_k)]$ at $r_k = n$ and $r_k = n+1$. Using the definition of $\psi(n)$, we can compute the difference of these two values as

$$[\psi(n+1) - \ln(n+1)] - [\psi(n) - \ln(n)] = \quad (27)$$

$$\frac{1}{n} - \ln(1 + \frac{1}{n}) > 0 \quad (28)$$

where the series expansion of $\ln(1+x)$ is used to get the inequality in RHS. This implies

$$[\psi(n+1) - \ln(n+1)] > [\psi(n) - \ln(n)]\,. \quad (29)$$

Therefore, we conclude that $[\psi(r_k) - \ln(r_k)]$ increases for increasing r_k and thus the maximum value of r_k (which is the full rank value) maximizes the first summation term in (15).

[2]This is widely known from existing literature, hence not shown in the figure.

Appendix B
Exact Capacity Equation (19)

In this section, we present the derivation steps leading to the exact capacity expression result in (19). From (18), define $C_k \triangleq \int_{-\infty}^{\infty} \log\left(1 + \frac{z}{\rho}\right) p_{z_k}(z) dz$. For $k \in \mathcal{I}_1$, substituting the value of $p_{z_k}(z)$, we get

$$C_k = \sum_{l=1}^{m} \sum_{i=1}^{\kappa_l} \frac{A_{li,k}}{\lambda_{l,k}^i \Gamma(i)} I_{li,k} \quad (30)$$

where

$$I_{li,k} \triangleq \int_0^{\infty} \log\left(1 + \frac{z}{\rho}\right) z^{i-1} e^{-\frac{z}{\lambda_{l,k}}} dz. \quad (31)$$

Then,

$$I_{li,k} = \left[\log(1+\frac{z}{\rho}) \int z^{i-1} e^{-\frac{z}{\lambda_{l,k}}} dz\right]_0^{\infty} - \frac{\log(e)}{\rho} \int_0^{\infty} \frac{\int z^{i-1} e^{-(\frac{z}{\lambda_{l,k}})} dz}{1+\frac{z}{\rho}} dz \quad (32)$$

Using $\int z^{i-1} e^{-\frac{z}{\lambda_{l,k}}} dz = \sum_{j=1}^{i} -\lambda_{l,k}^j z^{i-j} \frac{(i-1)!}{(i-j)!} e^{-\frac{z}{\lambda_{l,k}}}$ in (32), we get

$$I_{li,k} = \frac{\log(e)}{\rho} \sum_{j=1}^{i} \frac{(i-1)!}{(i-j)!} \lambda_{l,k}^j \underbrace{\int_0^{\infty} \frac{z^{i-j} e^{-\frac{z}{\lambda_{l,k}}}}{1+\frac{z}{\rho}} dz}_{S_{ijl,k}}. \quad (33)$$

Then we have

$$S_{ijl,k} = \rho e^{\frac{\rho}{\lambda_{l,k}}} \int_{\frac{\rho}{\lambda_{l,k}}}^{\infty} \frac{(t\lambda_{l,k} - \rho)^{i-j} e^{-t}}{t} dt =$$

$$\rho e^{\frac{\rho}{\lambda_{l,k}}} \sum_{q=0}^{i-j} (-1)^q \binom{i-j}{q} \lambda_{l,k}^{i-j-q} \rho^q \int_{\frac{\rho}{\lambda_{l,k}}}^{\infty} t^{i-j-q-1} e^{-t} dt \quad (34)$$

where we have used $t \triangleq \left(\frac{z}{\lambda_{l,k}} + \frac{\rho}{\lambda_{l,k}}\right)$ and the result $\frac{(t\lambda_{l,k}-\rho)^{i-j}}{t} = \sum_{q=0}^{i-j} (-1)^q \binom{i-j}{q} \lambda_{l,k}^{i-j-q} t^{i-j-q-1} \rho^q$ in simplifying the above. For $q \le i-j-1$, the integral in the RHS of (34) can be evaluated as

$$\int_{\frac{\rho}{\lambda_{l,k}}}^{\infty} t^{i-j-q-1} e^{-t} dt = \sum_{r=1}^{i-j-q} \left(\frac{\rho}{\lambda_{l,k}}\right)^{i-j-q-r} \frac{(i-j-q-1)!}{(i-j-q-r)!} e^{-\frac{\rho}{\lambda_{l,k}}} \quad (35)$$

while for $q = i-j$, we have

$$\int_{\frac{\rho}{\lambda_{l,k}}}^{\infty} t^{i-j-q-1} e^{-t} dt = \mathrm{E}_1(\frac{\rho}{\lambda_{l,k}}). \quad (36)$$

Using (35) and (36) in (34), we get the result in (21) and by using this result in (33), we get (20) and finally from (30), we get the first term of our capacity result in (19).

For $k \in \mathcal{I}_2$, using the pdf of Case II in Section III of [22], we have

$$C_k = \frac{\int_0^{\infty} \log\left(1+\frac{z}{\rho}\right) z^{r_k-1} e^{-\frac{z}{\lambda_{1,k}}} dz}{\lambda_{1,k}^{r_k} \Gamma(r_k)} = \frac{I_{1r_k,k}}{\lambda_{1,k}^{r_k} \Gamma(r_k)} \quad (37)$$

where $I_{1r_k,k}$ is given by (20). Therefore, summing up the above terms for $k \in \mathcal{I}_2$, we get the second term in (19) and hence our capacity result.

REFERENCES

[1] E. Telatar, "Capacity of multi-antenna Gaussian channels," *Eur. Trans. Telecommun.*, vol. 10, no. 6, pp. 585–595, 1999.

[2] M. Chiani, M. Win, and A. Zanella, "On the capacity of spatially correlated MIMO Rayleigh-fading channels," *IEEE Trans. Inf. Theory*, vol. 49, no. 10, pp. 2363–2371, Oct. 2003.

[3] H. Shin, M. Win, J. Lee, and M. Chiani, "On the capacity of doubly correlated MIMO channels," *IEEE Trans. Wireless Commun.*, vol. 5, no. 8, pp. 2253–2265, Aug. 2006.

[4] E. Yoon, J. Hansen, and A. Paulraj, "Space-frequency precoding with space-tap correlation information at the transmitter," *IEEE Trans. Commun.*, vol. 55, no. 9, pp. 1702 –1711, Sept. 2007.

[5] D. McNamara, M. Beach, and P. Fletcher, "Spatial correlation in indoor MIMO channels," in *Proc. IEEE Symp. Pers. Ind. Mobile Radio Commun (PIMRC)*, vol. 1, Sept. 2002, pp. 290–294.

[6] J. Kermoal, L. Schumacher, K. Pedersen, P. Mogensen, and F. Frederiksen, "A stochastic MIMO radio channel model with experimental validation," *IEEE J. Sel. Areas Commun.*, vol. 20, no. 6, pp. 1211–1226, Aug. 2002.

[7] A. Abdi and M. Kaveh, "A space-time correlation model for multielement antenna systems in mobile fading channels," *IEEE J. Sel. Areas Commun.*, vol. 20, no. 3, pp. 550–560, Apr. 2002.

[8] H. Ozcelik, M. Herdin, W. Weichselberger, J. Wallace, and E. Bonek, "Deficiencies of 'Kronecker' MIMO radio channel model," *IET Electron. Lett.*, vol. 39, no. 16, pp. 1209–1210, Aug. 2003.

[9] H. Bolcskei, D. Gesbert, and A. Paulraj, "On the capacity of OFDM-based spatial multiplexing systems," *IEEE Trans. Commun.*, vol. 50, no. 2, pp. 225–234, Feb. 2002.

[10] G. Taricco and E. Riegler, "On the ergodic capacity of correlated rician fading MIMO channels With Interference," *IEEE Trans. Inf. Theory*, vol. 57, no. 7, pp. 4123 –4137, July 2011.

[11] J. Dumont, W. Hachem, S. Lasaulce, P. Loubaton, and J. Najim, "On the capacity achieving covariance matrix for Rician MIMO channels: An Asymptotic Approach," *IEEE Trans. Inf. Theory*, vol. 56, no. 3, pp. 1048 –1069, March 2010.

[12] M. Matthaiou, G. Alexandropoulos, H. Q. Ngo, and E. Larsson, "Effective rate analysis of MISO Rician fading channels," in *Sensor Array and Multichannel Signal Processing Workshop (SAM) IEEE*, June 2012, pp. 53 –56.

[13] A. Bannour, M. Ammari, Y. Sun, and R. Bouallegue, "On the capacity of ASTC-MIMO-OFDM system in a correlated Rayleigh frequency-selective channel," in *Veh. Technol. Conf. (VTC Spring), IEEE*, May 2011, pp. 1–5.

[14] M. Chiani, M. Win, and H. Shin, "MIMO networks: The effects of interference," *IEEE Trans. Inf. Theory*, vol. 56, no. 1, pp. 336 –349, Jan. 2010.

[15] M. Vu, "MISO capacity with per-antenna power constraint," *IEEE Trans. Commun.*, vol. 59, no. 5, pp. 1268 –1274, May 2011.

[16] M. Codreanu, A. Tolli, M. Juntti, and M. Latva-aho, "MIMO downlink weighted sum rate maximization with power constraints per antenna groups," in *Veh. Technol. Conf. (VTC-Spring), IEEE*, Apr. 2007, pp. 2048 –2052.

[17] D. Qiao, M. Gursoy, and S. Velipasalar, "Transmission strategies in multiple-access fading channels with statistical QoS constraints," *IEEE Trans. Inf. Theory*, vol. 58, no. 3, pp. 1578 –1593, March 2012.

[18] V. Gottumukkala and H. Minn, "Capacity analysis and pilot-data power allocation for MIMO-OFDM with transmitter and receiver IQ imbalances and residual carrier frequency offset," *IEEE Trans. Veh. Technol.*, vol. 61, no. 2, pp. 553 –565, Feb. 2012.

[19] F. Oggier and B. Hassibi, "The secrecy capacity of the MIMO wiretap channel," *IEEE Trans. Inf. theory*, vol. 57, no. 8, pp. 4961 –4972, Aug. 2011.

[20] A. Ghaderipoor, C. Tellambura, and A. Paulraj, "On the application of character expansions for MIMO capacity analysis," *IEEE Trans. Inf. Theory*, vol. 58, no. 5, pp. 2950 –2962, May 2012.

[21] F. Dupuy and P. Loubaton, "On the capacity achieving covariance matrix for frequency selective MIMO channels using the asymptotic approach," *IEEE Trans. Inf. Theory*, vol. 57, no. 9, pp. 5737 –5753, Sept. 2011.

[22] Y. Li, H. Minn, and J. Zeng, "An average Cramer-Rao bound for frequency offset estimation in frequency-selective fading channels," *IEEE Trans. Commun.*, vol. 9, no. 3, pp. 871–875, March 2010.

[23] G. Raleigh and J. Cioffi, "Spatio-temporal coding for wireless communication," *IEEE Trans. Commun.*, vol. 46, no. 3, pp. 357–366, Mar. 1998.

[24] G. Raleigh and V. Jones, "Multivariate modulation and coding for wireless communication," *IEEE J. Sel. Areas Comm.*, vol. 17, no. 5, pp. 851–866, May 1999.

[25] D. Tse and P. Viswanath, *Fundamentals of wireless communication*. Cambridge Univ. Press, 2005.

[26] I. Gradshteyn, I. Ryzhik, A. Jeffrey, and D. Zwillinger, *Table of integrals, series, and products*. Academic press, 2007.

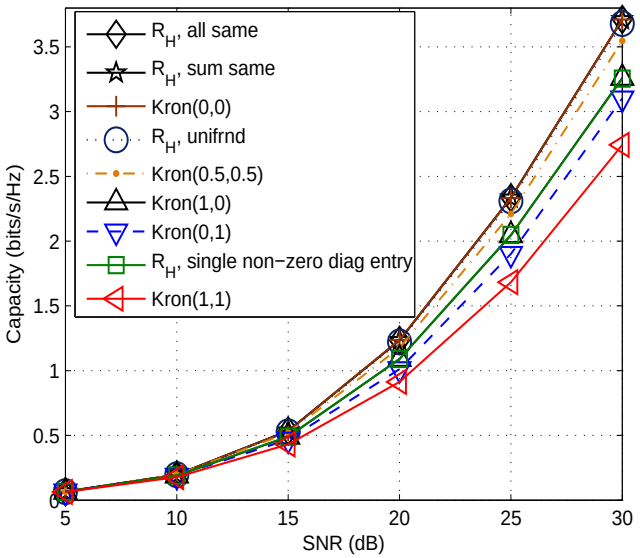

Fig. 1. Capacity comparison between arbitrary and Kronecker correlation models for SIMO-OFDM, $N = 64$, $L = M = 4$.

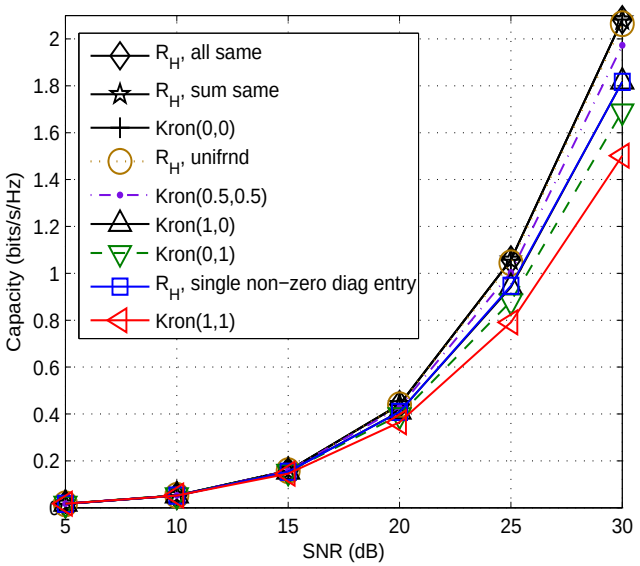

Fig. 2. Capacity comparison between arbitrary and Kronecker correlation models for MISO-OFDM, $N = 64$, $L = M = 4$.

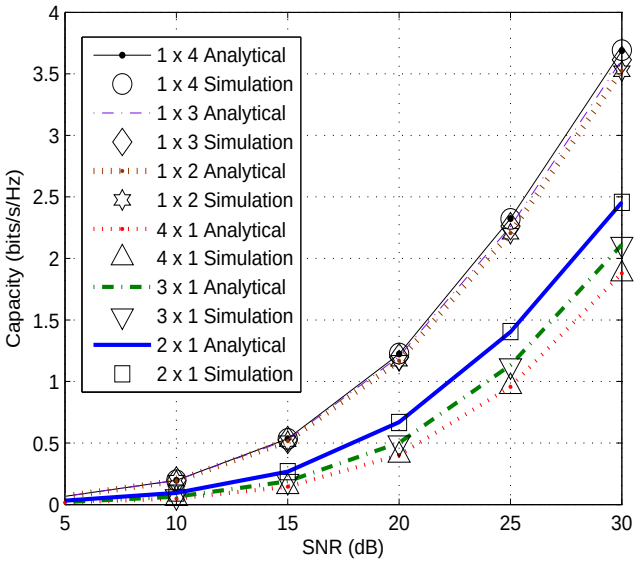

Fig. 3. Capacity comparison between analytical and simulation results for arbitrary correlation, $N = 64$, $L = 4$. In the legend, $1 \times x$ and $x \times 1$ refer to SIMO-OFDM and MISO-OFDM system, respectively, with $M = x$.

V. K. Varma Gottumukkala (S'13) received the B.Tech degree from the Indian Institute of Technology Delhi, India and a Masters degree in Electrical Engineering from Texas A&M University, College Station, Texas. He is currently pursuing the PhD degree in Electrical Engineering at the University of Texas at Dallas, Texas. His research interests are in the broad areas of wireless communications and networking.

Hlaing Minn (S'99, M'01, SM'07) received the B.E. degree in electrical & electronics engineering from the Yangon institute of Technology, Myanmar, in 1995, the M.Eng. degree in telecommunications from the Asian Institute of Technology (AIT), Thailand, in 1997, and the Ph.D. degree in electrical engineering from the University of Victoria, Canada, in 2001. He was a post-doctoral fellow at the University of Victoria during Jan.-Aug. 2002. He has been with the Erik Jonsson School of Engineering and Computer Science at the University of Texas at Dallas since Sept. 2002, and currently is an Associate Professor. His research interests include wireless communications, statistical signal processing, signal design, cross-layer design, and wireless health-care applications. Prof. Minn is an Editor for the IEEE Transactions on Communications and International Journal of Communications and Networks. He served as a Co-Chair of the Wireless Access Track in the IEEE VTC 2009 (Fall).